# Stabilization of a Fibronectin Type III Domain by the Removal of Unfavorable Electrostatic Interactions on the Protein Surface†

Akiko Koide, Michael R. Jordan, Scott R. Horner, Vincent Batori, and Shohei Koide*

*Department of Biochemistry and Biophysics, University of Rochester Medical Center, 601 Elmwood Avenue, Rochester, New York 14642*

*Received May 4, 2001; Revised Manuscript Received June 25, 2001*

ABSTRACT: It is generally considered that electrostatic interactions on the protein surface, such as ion pairs, contribute little to protein stability, although they may play important roles in conformational specificity. We found that the tenth fibronectin type III domain of human fibronectin (FNfn10) is more stable at acidic pH than neutral pH, with an apparent midpoint of transition near pH 4. Determination of p$K_a$'s for all the side chain carboxyl groups of Asp and Glu residues revealed that Asp 23 and Glu 9 have an upshifted p$K_a$. These residues and Asp 7 form a negatively charged patch on the surface of FNfn10, with Asp 7 centrally located between Asp 23 and Glu 9, suggesting repulsive electrostatic interactions among these residues at neutral pH. Mutant proteins, D7N and D7K, in which Asp 7 was replaced with Asn and Lys, respectively, exhibited a modest but significant increase in stability at neutral pH, compared to the wild type, and they no longer showed pH dependence of stability. The p$K_a$'s of Asp 23 and Glu 9 in these mutant proteins shifted closer to their respective unperturbed values, indicating that the unfavorable electrostatic interactions have been reduced in the mutant proteins. Interestingly, the wild-type and mutant proteins were all stabilized to a similar degree by the addition of 1 M sodium chloride at both neutral and acidic pH, suggesting that the repulsive interactions between the carboxyl groups cannot be effectively shielded by 1 M sodium chloride. These results indicate that repulsive interactions between like charges on the protein surface can destabilize a protein, and protein stability can be significantly improved by relieving these interactions.

Increasing the conformational stability of a protein by mutation is a major interest in protein design and biotechnology. The three-dimensional structures of proteins are stabilized by a combination of different types of forces. The hydrophobic effect, van der Waals interactions, and hydrogen bonds are known to contribute to stabilize the folded state of proteins (*1*−*3*). These stabilizing forces primarily originate from residues that are well packed in a protein, such as those that constitute the hydrophobic core. Because a change in the protein core would induce a rearrangement of adjacent moieties, it is difficult to improve protein stability by increasing these forces without massive computation (*4*). Ion pairs between charged groups are commonly found on the protein surface (*5*), and an ion pair could be introduced to a protein with small structural perturbations. However, a number of studies have demonstrated that the introduction of an attractive electrostatic interaction, such as an ion pair, on the protein surface has small effects on stability (*6, 7*). A large desolvation penalty and the loss of conformational entropy of amino acid side chains oppose the favorable electrostatic contribution (*8, 9*). Recent studies demonstrated that repulsive electrostatic interactions on the protein surface, in contrast, may significantly destabilize a protein, and that it is possible to improve protein stability by optimizing surface electrostatic interactions (*10*−*13*). In this article, we present another example of improving protein stability by modifying surface electrostatic interactions.

Fibronectin type III domain (FN3)[1] is a small $\beta$-sheet domain that is ubiquitously found in animal proteins (*14, 15*). The tenth FN3 from human fibronectin (FNfn10) is involved in the interaction between fibronectin and its cell-surface receptors, integrins (*16*), and it has been extensively studied as a prototype of FN3. Its three-dimensional structure has been determined (*17, 18*), and its conformational dynamics have been characterized in detail (*19*). Further, its stability and folding kinetics have been studied (*20*−*22*). These studies demonstrated that FNfn10 is an excellent system to investigate the relationships between structure, dynamics, and stability.

We have developed a protein engineering system using FNfn10 as a scaffold (*23*). In this system, surface loops of FNfn10 are diversified to generate combinatorial libraries, and FNfn10 mutants with novel functions, termed "monobodies", are selected using the phage-display technology. The excellent physical characteristics of FNfn10 allow us to introduce many mutations in these loops without disrupting its global fold. During the characterization of these mono-

† This work was supported by NIH Grant GM 55042 to S.K. M.R.J. was supported by the University of Rochester GEBS summer scholar program.

* Corresponding author. Phone: 1-716-275-8371. Fax: 1-716-275-6007. Email: shohei_koide@urmc.rochester.edu.

[1] Abbreviations: CD, circular dichroism; FN3, fibronectin type III domain; FNfn10, tenth FN3 of fibronectin; GuHCl, guanidine hydrochloride; HSQC, heteronuclear single-quantum correlation; NMR, nuclear magnetic resonance.

10.1021/bi010916y CCC: $20.00 
Published on Web 08/02/2001

bodies, we found that these proteins, as well as wild-type FNfn10, are significantly more stable at low pH than at neutral pH (*23*). These observations indicate that changes in the ionization state of some moieties in FNfn10 modulate the conformational stability of the protein, and suggest that it might be possible to enhance the conformational stability of FNfn10 at neutral pH by adjusting electrostatic properties of the protein. Improving the conformational stability of FNfn10 will also have practical importance, because of our interest in using FNfn10 as a scaffold in biotechnology applications.

In this study, we performed more detailed characterization of the pH dependence of FNfn10 stability, identified unfavorable interactions between side chain carboxyl groups, and improved the conformational stability of FNfn10 by point mutations on the surface. Our results demonstrate that the surface electrostatic interactions contribute significantly to protein stability, and it is possible to enhance protein stability by rationally modulating these interactions.

## EXPERIMENTAL PROCEDURES

*Protein Expression and Purification*. The wild-type protein used for the NMR studies contained residues 1−94 of FNfn10 [residue numbering is according to Figure 2(a) of Koide et al. (*23*)], and an additional two residues (Met-Gln) at the N-terminus (these two residues are numbered −2 and −1, respectively). The gene coding for the protein was inserted in pET3a (Novagen, WI). *Escherichia coli* BL21-(DE3) transformed with the expression vector was grown in the M9 minimal media supplemented with $^{13}$C-glucose and $^{15}$N-ammonium chloride (Cambridge Isotopes) as the sole carbon and nitrogen sources, respectively. Protein expression was induced as described previously (*23*). After harvesting the cells by centrifuge, the cells were lysed as described (*23*). After centrifugation, supernatant was dialyzed against 10 mM sodium acetate buffer (pH 5.0), the protein solution was applied to an SP-Sepharose FastFlow column (Amersham Pharmacia Biotech), and FN3 was eluted with a gradient of sodium chloride. The protein was concentrated using an Amicon concentrator using a YM-3 membrane (Millipore).

The wild-type protein used for the stability measurements contained an N-terminal his-tag (MGSSHHHHHHSS-GLVPRGSH) and residues −2 to 94 of FNfn10. The gene for FN3 described above was inserted in pET15b (Novagen). The protein was expressed and purified as described (*23*). The wild-type protein used for measurements of the pH dependence shown in Figure 1 contained Arg 6 to Thr mutation, which had originally been introduced to remove a secondary thrombin cleavage site (*23*). Because Asp 7, which is adjacent to Arg 6, was found to be critical in the pH dependence of FN3 stability as detailed under Results, subsequent studies were performed using the wild-type, Arg 6, background. The genes for the D7N and D7K mutants were constructed using standard polymerase chain reactions, and inserted in pET15b. These proteins were prepared in the same manner as for the wild-type protein. $^{13}$C,$^{15}$N-labeled proteins for p$K_a$ measurements were prepared as described above, and the his-tag moiety was not removed from these proteins.

*Chemical Denaturation Measurements*. Proteins were dissolved to a final concentration of 5 $\mu$M in 10 mM sodium citrate buffer at various pHs containing 100 mM sodium chloride. Guanidine hydrochloride (GuHCl)-induced unfolding experiments were performed as described previously (*23, 24*). GuHCl concentration was determined using an Abbe refractometer (Spectronic Instruments) as described (*25*). Data were analyzed according to the two-state model as described (*23, 26*).

*Thermal Denaturation Measurements*. Proteins were dissolved to a final concentration of 5 $\mu$M in 20 mM sodium phosphate buffer (pH 7.0) containing 0.1 or 1 M sodium chloride or in 20 mM glycine hydrochloride buffer (pH 2.4) containing 0.1 or 1 M sodium chloride. Additionally, 6.3 M urea was included in all solutions to ensure reversibility of the thermal denaturation reaction. In the absence of urea, we found that denatured FNfn10 adheres to the quartz surface, and that the thermal denaturation reaction was irreversible. Circular dichroism measurements were performed using a model 202 spectrometer equipped with a Peltier temperature controller (Aviv Instruments). A cuvette with a 0.5 cm path length was used. The ellipticity at 227 nm was recorded as the sample temperature was raised at a rate of approximately 1 °C/min. Because of the decomposition of urea at high temperature, the pH of protein solutions tended to shift upward during an experiment. We measured the pH of the protein solution before and after each thermal denaturation measurement to ensure that a shift of no more than 0.2 pH unit occurred in each measurement. At pH 2.4, two sections of a thermal denaturation curve (30−65 and 60−95 °C) were acquired from separate samples, to avoid a large pH shift. The thermal denaturation data were fit with the standard two-state model (*25*):

$$\Delta G(T) = \Delta H_m(1 - T/T_m) - \Delta C_p[(T_m - T) + T \ln (T/T_m)]$$

where $\Delta G(T)$ is the Gibbs free energy of unfolding at temperature $T$, $\Delta H_m$ is the enthalpy change upon unfolding at the midpoint of the transition, $T_m$, and $\Delta C_p$ is the heat capacity change upon unfolding. The value for $\Delta C_p$ was fixed at 1.74 kcal mol$^{-1}$ K$^{-1}$, according to the approximation of Myers et al. (*27*). Most of the data sets taken in the presence of 1 M NaCl did not have a sufficient baseline for the unfolded state, and thus we assumed the slope of the unfolded baseline in the presence of 1 M NaCl to be identical to that determined in the presence of 0.1 M NaCl.

*NMR Spectroscopy*. NMR experiments were performed at 30 °C on an INOVA 600 spectrometer (Varian Instruments). The C(CO)NH experiment (*28*) and the CBCACOHA experiment (*29*) were collected on a $^{13}$C,$^{15}$N-labeled wild-type FNfn10 sample (1 mM) dissolved in 50 mM sodium acetate buffer (pH 4.6) containing 5% (v/v) deuterium oxide, using a Varian 5 mm triple resonance probe with pulsed field gradient. The carboxyl $^{13}$C resonances were assigned based on the backbone $^{1}$H, $^{13}$C, and $^{15}$N resonance assignments of FNfn10 (S. Koide, unpublished data, and ref *30*). pH titration of carboxyl resonances was performed on a 0.3 mM FNfn10 sample dissolved in 10 mM sodium citrate containing 100 mM sodium chloride and 5% (v/v) deuterium oxide. An 8 mm triple resonance, pulsed field gradient probe (Nanolac Corp.) was used for pH titration. Two-dimensional H(C)-CO spectra were collected using the CBCACOHA pulse sequence as described previously (*31*). Sample pH was

changed by adding small aliquots of hydrochloric acid, and pH was measured before and after taking NMR data. $^{1}H,^{15}N$-HSQC spectra were taken as described previously (*32*). NMR data were processed using the NMRPipe package (*33*), and analyzed using the NMRView software (*34*).

NMR titration curves of the carboxyl $^{13}C$ resonances were fit to the Henderson−Hasselbalch equation to determine p$K_a$'s:

$$\delta(\mathrm{pH}) = (\delta_{\mathrm{acid}} + \delta_{\mathrm{base}}10^{(\mathrm{pH}-\mathrm{p}K_a)})/(1 + 10^{(\mathrm{pH}-\mathrm{p}K_a)})$$

where $\delta$ is the measured chemical shift, $\delta_{\mathrm{acid}}$ is the chemical shift associated with the protonated state, $\delta_{\mathrm{base}}$ is the chemical shift associated with the deprotonated state, and p$K_a$ is the p$K_a$ value for the residue. Data were also fit to an equation with two ionizable groups:

$$\delta(\mathrm{pH}) = (\delta_{\mathrm{AH2}} + \delta_{\mathrm{AH}}10^{(\mathrm{pH}-\mathrm{p}K_{a1})} + \delta_{\mathrm{A}}10^{(2\mathrm{pH}-\mathrm{p}K_{a1}-\mathrm{p}K_{a2})})/(1 + 10^{(\mathrm{pH}-\mathrm{p}K_{a1})} + 10^{(2\mathrm{pH}-\mathrm{p}K_{a1}-\mathrm{p}K_{a2})})$$

where $\delta_{\mathrm{AH2}}$, $\delta_{\mathrm{AH}}$, and $\delta_{\mathrm{A}}$ are the chemical shifts associated with the fully protonated, singularly protonated, and deprotonated states, respectively, and p$K_{a1}$ and p$K_{a2}$ are p$K_a$'s associated with the two ionization steps. Data fitting was performed using the nonlinear least-squares regression method in the program Igor Pro (WaveMetrics, OR) on a Macintosh computer.

## RESULTS

*pH Dependence of FNfn10 Stability*. In our previous study, we found that FNfn10 is more stable at acidic pH than at neutral pH (*23*). In this study we further characterized the pH dependence of its stability. Because of its high stability, FNfn10 could not be fully denatured in urea at 30 °C. Thus, we used GuHCl-induced chemical denaturation (Figure 1). The denaturation reaction was fully reversible under all conditions tested. To minimize errors caused by extrapolation, the free energy of unfolding at 4 M GuHCl was used for comparison (Figure 1). The stability increased as the pH was lowered, with apparent plateaus at both ends of the pH range. The pH dependence curve has an apparent transition midpoint near pH 4. In addition, we noted a gradual increase in the *m* value, the dependence of the unfolding free energy on denaturant concentration. Pace et al. reported a similar pH dependence of the *m* value for barnase (*35*). These results indicate that FNfn10 contains interactions that stabilize the protein at low pH, or those that destabilize it at neutral pH. The results also suggest that by identifying and altering the interactions that give rise to the pH dependence, one may be able to improve the stability of FNfn10 at neutral pH to a degree similar to that found at low pH.

*Determination of p$K_a$'s of the Side Chain Carboxyl Groups in Wild-Type FNfn10*. The pH dependence of FNfn10 stability suggests that amino acids with p$K_a$ near 4 are involved in the observed transition. The carboxyl groups of Asp and Glu generally have a p$K_a$ in this range (*5*). It is well-known that if a carboxyl group has unfavorable (i.e., destabilizing) interactions in the folded state, its p$K_a$ is shifted to a higher value from its unperturbed value (*8*). If a carboxyl group has favorable interactions in the folded state, it has a lower p$K_a$. Thus, we determined the p$K_a$ values of all

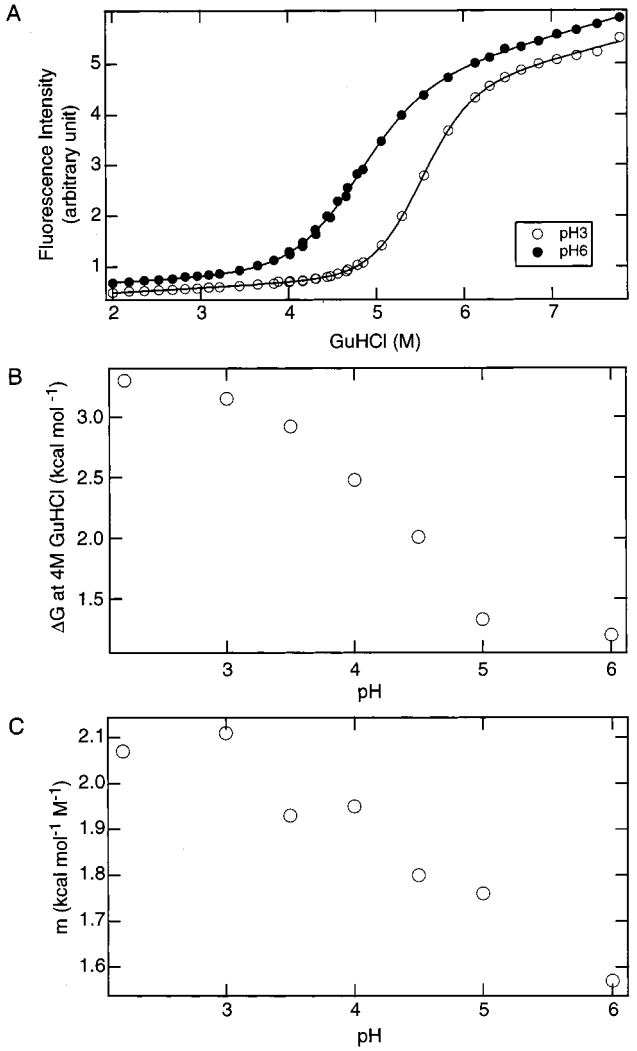


FIGURE 1: (A) Guanidine hydrochloride (GuHCl)-induced denaturation of FNfn10 monitored by Trp fluorescence. The fluorescence emission intensity at 355 nm is shown as a function of GuHCl concentration. The lines show the best fits of the data to the two-state transition model. (B) Stability of FN3 at 4 M GuHCl plotted as a function of pH. (C) pH dependence of the *m* value.

carboxylates in FNfn10 using heteronuclear NMR spectroscopy, to identify stabilizing and destabilizing interactions involving carboxyl groups.

First, we assigned the $^{13}C$ resonance for the carboxyl carbon of each Asp and Glu residue in FNfn10 (Figure 2). Next we performed pH titration of the $^{13}C$ resonances for these groups (Figure 3). Titration curves for Asp 3, 67, and 80 and for Glu 38 and 47 could be fit well with the Henderson−Hasselbalch equation with a single p$K_a$. The p$K_a$ values for these residues (Table 1) are either close to or slightly lower than their respective unperturbed values [3.8−4.1 for Asp, and 4.1−4.6 for Glu (*36*)], indicating that these carboxyl groups are involved in neutral or slightly favorable electrostatic interactions in the folded state.

The titration curves for Asp 7 and 23 and for Glu 9 were fit better with the Henderson−Hasselbalch equation with two p$K_a$ values, and one of the two p$K_a$ values for each was shifted higher than the respective unperturbed values (Figure 3B). The titration curves with two apparent p$K_a$ values of these carboxyl groups may be due to the influence of an ionizable group in the vicinity. In the three-dimensional

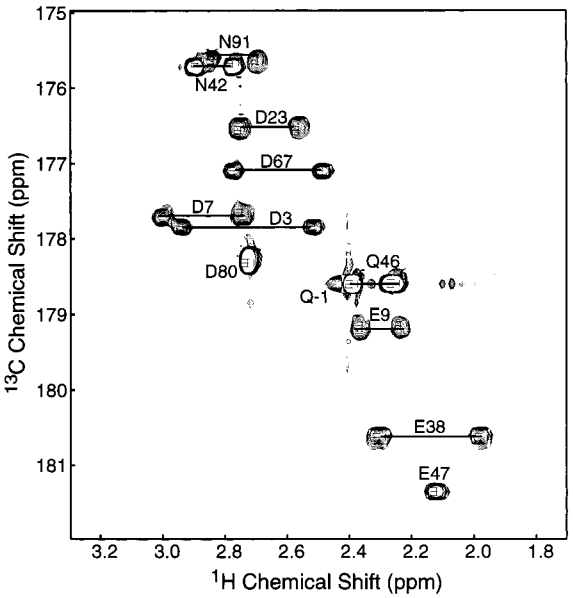


FIGURE 2: Two-dimensional H(C)CO spectrum of FNfn10 showing the $^{13}$C chemical shift of the carboxyl carbon (vertical axis) and the $^{1}$H shift of $^{1}H^{\beta}$ of Asp or $^{1}H^{\gamma}$ of Glu, respectively (horizontal axis). Cross-peaks are labeled with their respective residue numbers.

structure of FNfn10 (*17*), Asp 7 and 23, and Glu 9 form a patch on the surface (Figure 4), with Asp 7 centrally located in the patch. Thus, it is reasonable to expect that these residues influence each other's ionization profile. To identify which of the three residues has a highly upshifted p$K_a$, we then collected the H(C)CO spectrum of the protein in 99% $D_2O$ buffer at pH* 5.0 (direct pH meter reading). Asp 23 and Glu 9 showed larger deuterium isotope shifts (0.33 and 0.32 ppm, respectively) than Asp 7 (0.18 ppm). These results show that Asp 23 and Glu 9 are protonated to a greater degree than Asp 7. Thus, we concluded that Asp 23 and Glu 9 have highly upshifted p$K_a$'s, due to the strong influence of Asp 7.

*Mutational Analysis*. The spatial proximity of Asp 7 and 23, and Glu 9 explains the unfavorable electrostatic interactions in FNfn10 identified in this study. At low pH where these residues are protonated and neutral, the repulsive interactions are expected to be mostly relieved. Thus, it should be possible to improve the stability of FNfn10 at neutral pH, by removing the electrostatic repulsion between these three residues. Because Asp 7 is centrally located among the three residues, we decided to mutate Asp 7. We prepared two mutants, D7N and D7K. The former neutralizes the negative charge with a residue of virtually identical size. The latter places a positive charge at residue 7 and increases the size of the side chain.

The $^{1}$H,$^{15}$N-HSQC spectra of the two mutant proteins were nearly identical to that of the wild-type protein, indicating that these mutations did not cause large structural perturbations (data not shown). The degrees of stability of the mutant proteins were then characterized using thermal and chemical denaturation measurements. Thermal denaturation measurements were performed initially with 100 mM sodium chloride, and 6.3 M urea was included to ensure reversible denaturation and to decrease the temperature of the thermal transition. All the proteins were predominantly folded in 6.3 M urea at room temperature. All the proteins underwent a cooperative transition, and the two mutants were found to

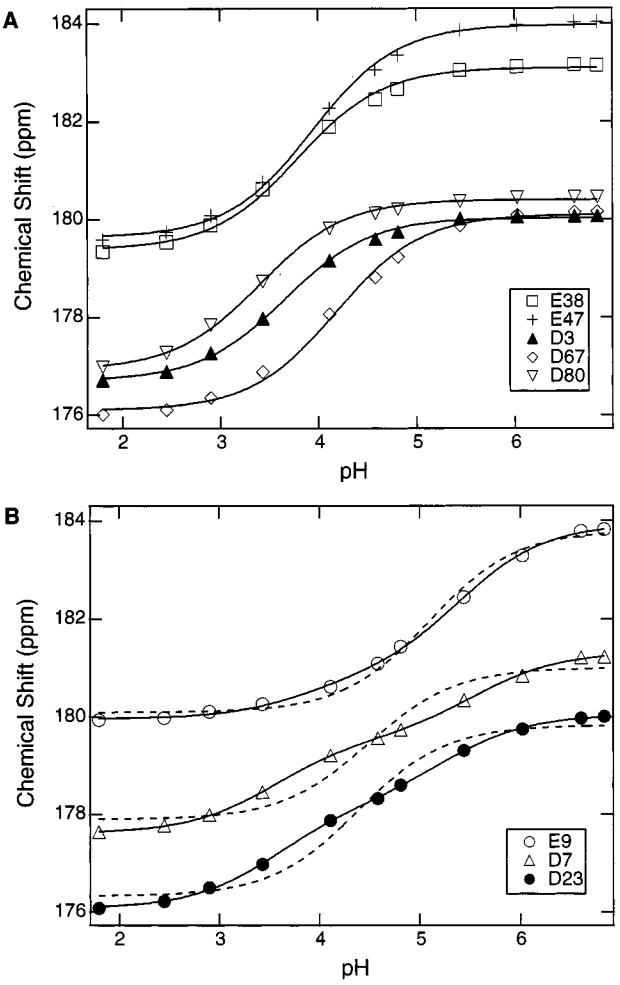


FIGURE 3: pH-dependent shifts of the $^{13}$C chemical shifts of the carboxyl carbons of Asp and Glu residues in FNfn10. Panel A shows data for Asp 3, 67, and 80, and for Glu 38 and 47. The lines are the best fits of the data to the Henderson−Hasselbalch equation with one ionizable group (*31*). Panel B shows data for Asp 7 and 23 and for Glu 9. The continuous lines show the best fits to the Henderson−Hasselbalch equation with two ionizable groups, while the dashed lines show the best fits to the equation with a single ionizable group.

Table 1: p$K_a$ Values for Asp and Glu Residues in FN3[a]

| | protein | | |
|---|---|---|---|
| residue | wild-type | D7N | D7K |
| E9 | 3.84, 5.40[b] | 4.98 | 4.53 |
| E38 | 3.79 | 3.87 | 3.86 |
| E47 | 3.94 | 3.99 | 3.99 |
| D3 | 3.66 | 3.72 | 3.74 |
| D7 | 3.54, 5.54[b] | – | – |
| D23 | 3.54, 5.25[b] | 3.68 | 3.82 |
| D67 | 4.18 | 4.17 | 4.14 |
| D80 | 3.40 | 3.49 | 3.48 |

[a] The standard deviations in the p$K_a$ values are less than 0.05 pH unit for those fit with a single p$K_a$ and less than 0.15 pH unit for those with two p$K_a$'s. [b] Data for E9, D7, and D23 were fit with a transition curve with two p$K_a$ values.

be significantly more stable than the wild type at neutral pH (Figure 5 and Table 2). Furthermore, these mutations almost eliminated the pH dependence of the conformational stability of FNfn10. These results confirmed that destabilizing interactions involving Asp 7 in wild-type FNfn10 at neutral pH are the primary cause of the pH dependence.

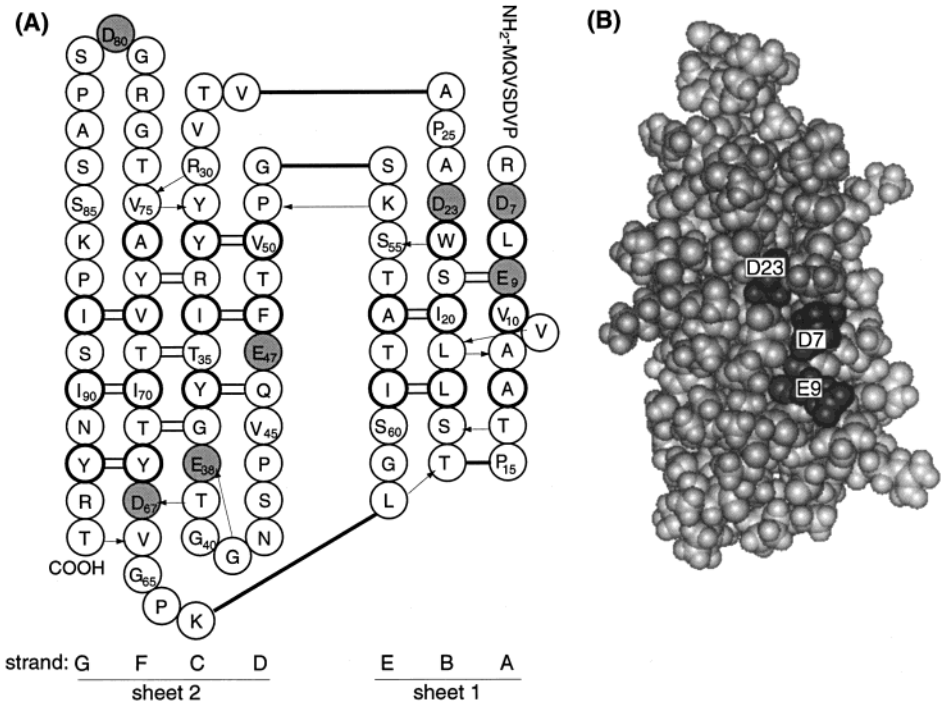


FIGURE 4: (A) Amino acid sequence of FNfn10 shown according to its topology (*17*). Asp and Glu residues are highlighted with gray circles. The thin lines and arrows connecting circles indicate backbone hydrogen bonds. (B) CPK model of FN3 showing the locations of Asp 7 and 23 and Glu 9.

We then investigated the effect of increased sodium chloride concentration on the conformational stability of the wild-type and the two mutant proteins. All proteins were more stable in 1 M sodium chloride than in 0.1 M sodium chloride (Figure 5). The increase of the sodium chloride concentration elevated the $T_m$ of the mutant proteins by approximately 10 °C at both acidic and neutral pH (Table 2). Remarkably, the wild-type protein was also equally stabilized at both pHs, although it contains unfavorable interactions among the carboxyl groups at neutral pH but not at acidic pH.

Chemical denaturation of FNfn10 proteins was monitored using fluorescence emission from the single Trp residue of FNfn10 (Figure 6). The free energies of unfolding at pH 6.0 and 4 M GuHCl were determined to be 1.1 (±0.3), 1.7 (±0.2), and 1.4 (±0.1) kcal/mol for the wild type, D7N, and D7K, respectively, indicating that the two mutations also increased the conformational stability against chemical denaturation.

*Determination of the p$K_a$'s of the Side Chain Carboxyl Groups in the Mutant Proteins*. We then investigated the ionization properties of carboxyl groups in the two mutant proteins. The 2D H(C)CO spectra of the mutant proteins at the high and low ends of the pH titration (pH ∼7 and ∼1.5, respectively) were nearly identical to the respective spectra of the wild type, except for the loss of the cross-peaks for Asp 7 (data not shown). This similarity allowed us to unambiguously assign resonances of the mutants, based on the assignments for wild-type FNfn10. The pH titration experiments revealed that, except for Glu 9 and Asp 23, the behaviors of Asp and Glu carboxyl groups are very close to their counterparts in the wild-type protein (Figure 7 , panels A, C, D, F, and G, and Table 1), indicating that the two mutations have marginal effects on the electrostatic environments for these carboxylates. In contrast, the titration curves

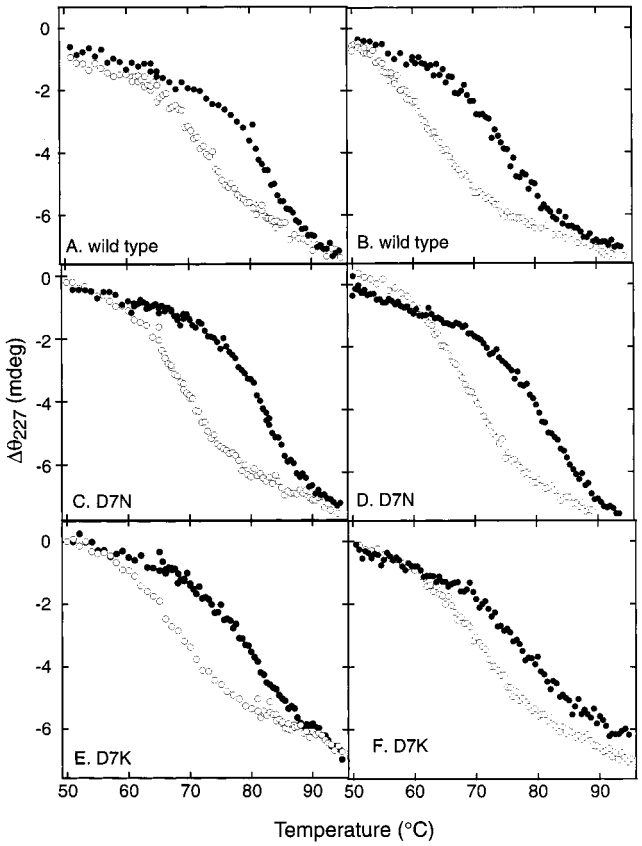


FIGURE 5: Thermal denaturation of the wild-type and mutant FNfn10 proteins at pH 7.0 and 2.4 in the presence of 6.3 M urea and 0.1 or 1.0 M NaCl. The change in the circular dichroism signal at 227 nm is plotted as a function of temperature. The filled circles show the data in the presence of 1 M NaCl, and the open circles are the data in the presence of 0.1 M NaCl. The left column shows data taken at pH 2.4 and the right column at pH 7.0. The identity of proteins is indicated in the panels.

Table 2: Midpoint of Thermal Denaturation (in °C) of Wild-Type and Mutant FN3 in the Presence of 6.3 M Urea[a]

| | pH 2.4 | | pH 7.0 | |
|---|---|---|---|---|
| protein | 0.1 M NaCl | 1 M NaCl | 0.1 M NaCl | 1 M NaCl |
| wild type | 72 | 82 | 62 | 70 |
| D7N | 68 | 82 | 69 | 80 |
| D7K | 69 | 77 | 70 | 78 |

[a] The error in the midpoints for the 0.1 M NaCl data is ±0.5 °C. Because most of the 1 M NaCl data did not have a sufficient baseline for the denatured state, we estimate the error in the midpoints for these data to be ±2 °C.

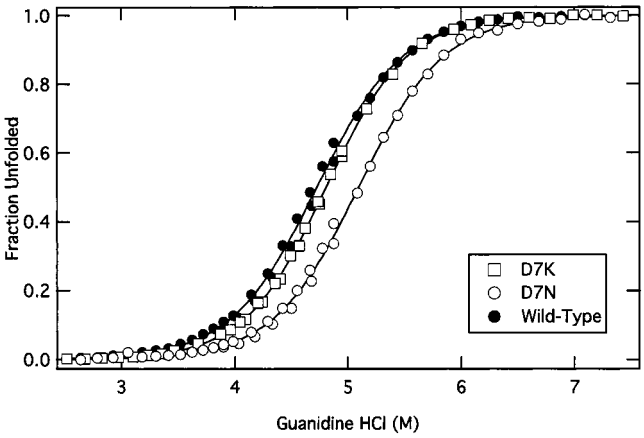


FIGURE 6: GuHCl-induced denaturation of FNfn10 mutants monitored with fluorescence. Fluorescence data (similar to Figure 1A) were converted to the fraction of unfolded protein according to the two-state transition model (*10*), and plotted as a function of [GuHCl].

for E9 and D23 show significant changes upon mutation (Figure 7, panels B and E). The p$K_a$ of D23 was lowered by more than 1.6 and 1.4 pH units in the D7N and D7K mutants, respectively. These results clearly show that the repulsive interaction between D7 and D23 contributes to the increase in p$K_a$ of Asp 23 in the wild-type protein, and that it was eliminated by the neutralization of the negative charge at residue 7. The p$K_a$ of Glu 9 was reduced by 0.4 pH unit by the D7N mutation, while it was decreased by 0.8 pH unit in the D7K mutant. The greater reduction of Glu 9 p$K_a$ by the D7K mutation suggests that there may be a favorable interaction between Lys 7 and Glu 9 in this mutant protein.

## DISCUSSION

We have identified unfavorable electrostatic interactions in FNfn10, and improved its conformational stability by mutations on the protein surface. Our results demonstrate that repulsive interactions between like charges on the protein surface significantly destabilize a protein. Our results are also consistent with recent reports by other groups (*10*−*13*), in which protein stability was improved by eliminating unfavorable electrostatic interactions on the surface. In these studies, candidates for mutations were identified by electrostatic calculations (*10, 12, 13*) or by sequence comparison of homologous proteins with different stability (*11*). Our strategy using p$K_a$ determination using NMR has both advantages and disadvantages over the other strategies. Our method directly identifies residues that destabilize a protein. Also it does not depend on the availability of the high-resolution structure of the protein of interest. Electrostatic

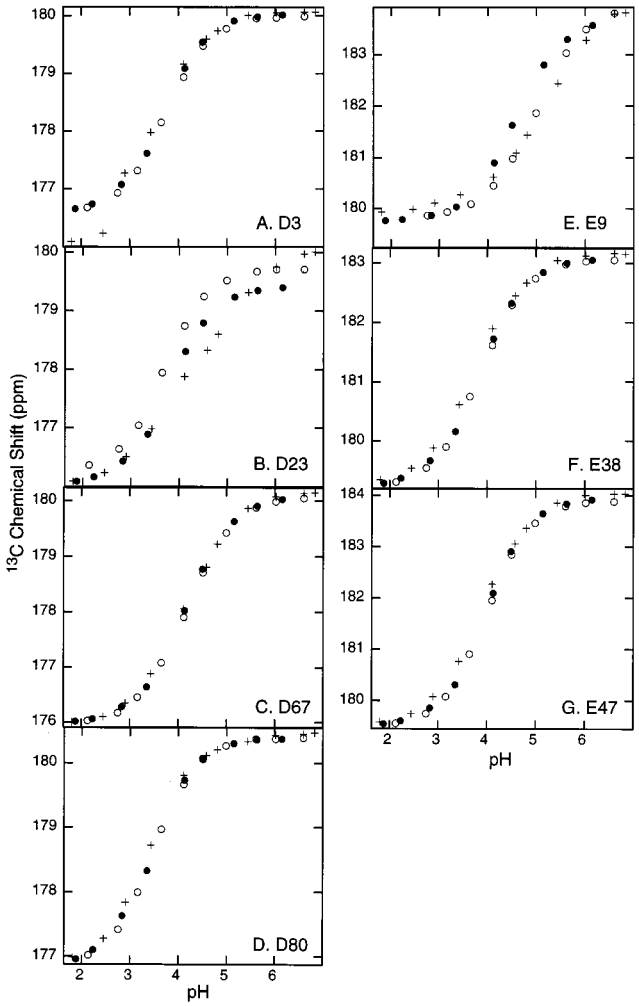


FIGURE 7: pH titration of the carboxyl $^{13}$C resonance of Asp and Glu residues in D7N (open circles) and D7K (closed circles) FNfn10. Data for the wild-type (crosses) are also shown for comparison. Residue names are denoted in the individual panels.

calculations may have large errors due to the flexibility of amino acid side chains on the surface, and the uncertainty in the dielectric constant on the protein surface and in the protein interior. For example, in the NMR structure of FNfn10 (*17*), the root-mean-squared deviations among 16 model structures for the $O^{\epsilon}$ atom of Glu residues are 1.2−2.4 Å, and those for Lys $N^{\zeta}$ atoms are 1.5−3.1 Å. Such uncertainties in atom position can potentially cause large differences in calculation results. On the other hand, our strategy requires the NMR assignments for carboxyl residues, and NMR measurements over a wide pH range. Although recent advances in NMR spectroscopy have made it straightforward to obtain resonance assignments for a small protein, some proteins may not be sufficiently soluble over the desired pH range. In addition, knowledge of the p$K_a$ values of ionizable groups in the denatured state is necessary for accurately evaluating contributions of individual residues to stability (*8*). Kuhlman et al. (*36*) showed that p$K_a$'s of carboxylates in the denatured state have a considerably larger range than those obtained from small model compounds. Despite these limitations, our method should be applicable to many proteins.

We showed that the unfavorable interactions involving the carboxyl groups of Asp 7, Glu 9, and Asp23 were no longer

present if these groups were protonated at low pH or if Asp 7 was replaced with Asn or Lys. The similarity in the measured stability of the mutants and the wild type at low pH (Table 2) suggests that no other factors significantly contribute to the pH dependence of FNfn10 stability and that the mutations caused minimal structural perturbations. The little structural perturbation was expected, since the carboxyl groups of these three residues are at least 50% exposed to the solvent, based on the solvent-accessible surface area calculation on the NMR structure (*17*).

The difference in thermal stability of the wild-type protein between acidic and neutral pH persisted in 1 M sodium chloride (Table 2). Likewise, the wild-type protein exhibited a large pH dependence in stability in 4 M GuHCl (Figure 1). Furthermore, upon the increase in the sodium chloride concentration from 0.1 to 1.0 M, the $T_m$ of the wild-type and mutant proteins all increased by ~10 °C, which is the same magnitude as the change in $T_m$ of the wild type by the pH shift. These data indicate that the unfavorable interactions identified in this study were not effectively shielded in 1 M NaCl or in 4 M GuHCl. Because the effect of increased sodium chloride was uniform, this stabilization effect of sodium chloride is likely due to the nonspecific salting-out effect (*37*). Other groups also reported little shielding effect of salts on electrostatic interactions (*38*, *39*). Electrostatic interactions are often thought to diminish with increasing ionic strength, particularly if the site of interaction is highly exposed. Accordingly, our data at neutral pH (Table 2) showing no difference in the salt sensitivity between the wild type and the mutants could be interpreted as Asp 7 not being responsible for destabilizing electrostatic interactions. Although the reason for this salt insensitivity is not yet clear, our results provide a cautionary note on concluding the presence and absence of electrostatic interactions solely based on salt concentration dependence.

The carboxyl triad (Asp 7 and 23, and Glu 9) is highly conserved in FNfn10 from nine different organisms that were available in the protein sequence databank at the National Center for Biotechnology Information (www.ncbi.nlm.nih.gov). In these FNfn10 sequences, Asp 9 is conserved except for one case where it is replaced with Asn, and Glu 9 is completely conserved. The position 23 is either Asp or Glu, preserving the negative charge. As we discovered in this study, the interactions among these residues are destabilizing. Thus, their high conservation, despite their negative effects on stability, suggests that these residues have functional importance in the biology of fibronectin. In the structure of a four-FN3 segment of human fibronectin (*40*), these residues are not directly involved in interactions with adjacent domains. Also these residues are located on the opposite face of FNfn10 from the integrin binding RGD sequence in the FG loop (Figure 4). Therefore, it is not clear why these destabilizing residues are almost completely conserved in FNfn10. In contrast, no other FN3 domains in human fibronectin contain this carboxyl triad (for a sequence alignment, see ref *17*). The carboxyl triad of FNfn10 may be involved in important interactions that have not been identified to date.

Clarke et al. (*41*) reported that the stability of the third FN3 of human tenascin (TNfn3) increased as the pH was decreased from 7 to 5. Although they could not perform stability measurements below pH 5 due to protein aggregation, the pH dependence of TNfn3 resembles that of FNfn10 shown in Figure 1. TNfn3 does not contain the carboxylate triad at positions corresponding to residues 7, 9, and 23 of FNfn10 (*42*), indicating that the destabilization of TNfn3 at neutral pH is caused by a different mechanism from that for FNfn10. A visual inspection of the TNfn3 structure revealed that it has a large number of carboxyl groups, and that Glu 834 and Asp 850 (numbering according to ref *42*) forms a cross-strand pair. It will be interesting to examine whether altering this pair can increase the stability of TNfn3.

In conclusion, we have described a strategy to experimentally identify unfavorable electrostatic interactions on the protein surface and improve the protein stability by relieving such interactions. Our results have demonstrated that forming a repulsive interaction between carboxyl groups significantly destabilizes a protein. This is in contrast to the small contributions of forming a solvent-exposed ion pair. Unfavorable electrostatic interactions on the surface seem quite common in natural proteins. Therefore, optimization of the surface electrostatic properties may be a generally applicable strategy for increasing protein stability (*10*−*13*). In addition, repulsive interactions between carboxylates may be exploited for destabilizing undesirable, alternate conformations in protein design ("negative design").

## ACKNOWLEDGMENT

We thank Dr. L. E. Kay for NMR pulse sequences, Dr. L. P. McIntosh for advice on NMR measurements, Dr. D. P. Raleigh for helpful discussions, Dr. S. D. Kennedy for assistance in NMR experiments, and F. Gruswitz for critical reading of the manuscript.

## REFERENCES

1. Kauzmann, W. (1959) *Adv. Protein Chem. 14*, 1−63.
2. Dill, K. A. (1990) *Biochemistry 29*, 7133−7155.
3. Pace, C. N., Shirley, B. A., McNutt, M., and Gajiwala, K. (1996) *FASEB J. 10*, 75−83.
4. Malakauskas, S. M., and Mayo, S. L. (1998) *Nat. Struct. Biol. 5*, 470−475.
5. Creighton, T. E. (1993) *Proteins: structures and molecular properties*, Freeman, New York.
6. Dao-pin, S., Sauer, U., Nicholson, H., and Matthews, B. W. (1991) *Biochemistry 30*, 7142−7153.
7. Sali, D., Bycroft, M., and Fersht, A. R. (1991) *J. Mol. Biol. 220*, 779−788.
8. Yang, A.-S., and Honig, B. (1992) *Curr. Opin. Struct. Biol. 2*, 40−45.
9. Hendsch, Z. S., and Tidor, B. (1994) *Protein Sci. 3*, 211−226.
10. Loladze, V. V., Ibarra-Molero, B., Sanchez-Ruiz, J. M., and Makhatadze, G. I. (1999) *Biochemistry 38*, 16419−16423.
11. Perl, D., Mueller, U., Heinemann, U., and Schmid, F. X. (2000) *Nat. Struct. Biol. 7*, 380−383.
12. Spector, S., Wang, M., Carp, S. A., Robblee, J., Hendsch, Z. S., Fairman, R., Tidor, B., and Raleigh, D. P. (2000) *Biochemistry 39*, 872−879.
13. Grimsley, G. R., Shaw, K. L., Fee, L. R., Alston, R. W., Huyghues-Despointes, B. M., Thurlkill, R. L., Scholtz, J. M., and Pace, C. N. (1999) *Protein Sci. 8*, 1843−1849.
14. Bork, P., and Doolittle, R. F. (1992) *Proc. Natl. Acad. Sci. U.S.A. 89*, 8990−8994.
15. Baron, M., Norman, D. G., and Campbell, I. D. (1991) *Trends Biochem. Sci. 16*, 13−17.
16. Pierschbacher, M. D., and Ruoslahti, E. (1984) *Nature 309*, 30−33.
17. Main, A. L., Harvey, T. S., Baron, M., Boyd, J., and Campbell, I. D. (1992) *Cell 71*, 671−678.

18. Dickinson, C. D., Veerapandian, B., Dai, X.-P., Hamlin, R. C., Xuong, N.-H., Ruoslahti, E., and Ely, K. R. (1994) *J. Mol. Biol. 236*, 1079−1092.
19. Carr, P. A., Erickson, H. P., and Palmer, A. G. R. (1997) *Structure 5*, 949−959.
20. Plaxco, K. W., Spitzfaden, C., Campbell, I. D., and Dobson, C. M. (1996) *Proc. Natl. Acad. Sci. U.S.A. 93*, 10703−10706.
21. Plaxco, K. W., Spitzfaden, C., Campbell, I. D., and Dobson, C. M. (1997) *J. Mol. Biol. 270*, 763−770.
22. Cota, E., and Clarke, J. (2000) *Protein Sci. 9*, 112−120.
23. Koide, A., Bailey, C. W., Huang, X., and Koide, S. (1998) *J. Mol. Biol. 284*, 1141−1151.
24. Koide, S., Bu, Z., Risal, D., Pham, T.-N., Nakagawa, T., Tamura, A., and Engelman, D. M. (1999) *Biochemistry 38*, 4757−4767.
25. Pace, C. N., and Sholtz, J. M. (1997) in *Protein structure. A practical approach* (Creighton, T. E., Ed.) pp 299−321, IRL Press, Oxford.
26. Santoro, M. M., and Bolen, D. W. (1988) *Biochemistry 27*, 8063−8068.
27. Myers, J. K., Pace, C. N., and Scholtz, J. M. (1995) *Protein Sci. 4*, 2138−2148.
28. Grzesiek, S., Anglister, J., and Bax, A. (1993) *J. Magn. Reson. B 101*, 114−119.
29. Kay, L. E. (1993) *J. Am. Chem. Soc. 115*, 2055−2057.
30. Baron, M., Main, A. L., Driscoll, P. C., Mardon, H. J., Boyd, J., and Campbell, I. D. (1992) *Biochemistry 31*, 2068−2073.
31. McIntosh, L. P., Hand, G., Johnson, P. E., Joshi, M. D., Koerner, M., Plesniak, L. A., Ziser, L., Wakarchuk, W. W., and Withers, S. G. (1996) *Biochemistry 35*, 9958−9966.
32. Kay, L. E., Keifer, P., and Saarinen, T. (1992) *J. Am. Chem. Soc. 114*, 10663−10665.
33. Delaglio, F., Grzesiek, S., Vuister, G. W., Zhu, G., Pfeifer, J., and Bax, A. (1995) *J. Biomol. NMR 6*, 277−293.
34. Johnson, B. A., and Blevins, R. A. (1994) *J. Biomol. NMR 4*, 603−614.
35. Pace, C. N., Laurents, D. V., and Erickson, R. E. (1992) *Biochemistry 31*, 2728−2734.
36. Kuhlman, B., Luisi, D. L., Young, P., and Raleigh, D. P. (1999) *Biochemistry 38*, 4896−4903.
37. Timasheff, S. N. (1992) *Curr. Opin. Struct. Biol. 2*, 35−39.
38. Perutz, M. F., Gronenborn, A. M., Clore, G. M., Fogg, J. H., and Shih, D. T. (1985) *J. Mol. Biol. 183*, 491−498.
39. Hendsch, Z. S., Jonsson, T., Sauer, R. T., and Tidor, B. (1996) *Biochemistry 35*, 7621−7625.
40. Leahy, D. J., Aukhil, I., and Erickson, H. P. (1996) *Cell 84*, 155−164.
41. Clarke, J., Hamill, S. J., and Johnson, C. M. (1997) *J. Mol. Biol. 270*, 771−778.
42. Leahy, D. J., Hendrickson, W. A., Aukhil, I., and Erickson, H. P. (1992) *Science 258*, 987−991.

BI010916Y